Acta Cryst E CRYSTALLOGRAPHIC COMMUNICATIONS

ISSN 2056-9890

Occupational disorder of cobalt and indium in the crystal structure of $Co_5In_3SbSi_2O_{16}$

Tobias Wolflehner and Matthias Weil*

Institute for Chemical Technologies and Analytics, Division of Applied Solid State Chemistry, Getreidemarkt 9/E164-05-1, 1060 Vienna, Austria. *Correspondence e-mail: matthias.weil@tuwien.ac.at

Received 8 October 2026
Accepted 21 October 2026

Edited by W. T. A. Harrison, University of Aberdeen, United Kingdom

Keywords: crystal structure; co-occupation; isotypism; framework structure; structure comparison.

CCDC reference: 2597010

Supporting information: this article has supporting information at journals.iucr.org/e

Pentacobalt(II) triindium(III) antimony(V) disilicon(VI) hexadecaoxide, $Co_5In_3SbSi_2O_{16}$, was obtained as a single-crystalline by-product through a reaction with the silica glass ampoule during a chemical vapor transport reaction. It crystallizes isotypically with $Co_8TeAs_2O_{16}$ in space group *Cmce*, with two (out of four) Co sites co-occupied by In, the Te site replaced by Sb, and the As site replaced by Si. The crystal structure of $Co_5In_3SbSi_2O_{16}$ consists of [CoO_6], [(In,Co)O_6], and [SbO_6] octahedra, and [CoO_4] and [SiO_4] tetrahedra, fused by vertex- and edge-sharing into a complex three-dimensional framework.

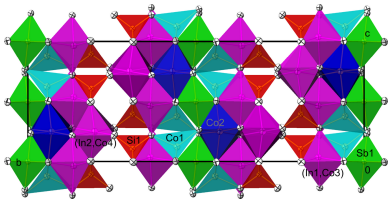
1. Chemical context

First-row divalent transition-metal (M^{II}) antimonates with composition M_2InSbO_6 have a corundum-related crystal structure and exhibit interesting magnetic properties, including frustrated magnetism for Mn_2InSbO_6 (Ivanov *et al.*, 2011), long-range incommensurate antiferromagnetic order at low temperatures for Ni_2InSbO_6 (Ivanov *et al.*, 2013), or, depending on the modification of Co_2InSbO_6, a sharp ferrimagnetic transition at 65 K (Ji *et al.*, 2022). The relevant materials were produced as powder samples *via* solid-state reactions, either at normal pressure (M = Ni, Mn) or under high-pressure conditions (M = Co). Since chemical vapour transport reactions (Binnewies *et al.*, 2012) had been successfully applied for single crystal growth of Ni_2InSbO_6 in the millimetre size range (Weil *et al.*, 2014), an attempt was made to apply this method to crystal growth of Co_2InSbO_6. The crystals obtained during one of these experiments did not have the desired composition, but also contained silicon as an additional element, which resulted from a reaction with the silica glass ampoule. This article reports on the corresponding crystal structure of $Co_5In_3SbSi_2O_{16}$, (**I**).

2. Structural commentary

Compound (**I**) is isotypic with $Co_8TeAs_2O_{16}$ (Staack & Müller-Buschbaum, 1997). It comprises two Co sites (Co1: multiplicity 8, Wyckoff letter *f*, site symmetry *m*..; Co2: 8 *e*, .2.), two mixed-occupied (In/Co) sites (In1/Co3: 8 *f*; In2/Co4: 8 *e*), one Si (Si1: 8 *f*), one Sb (Sb1: 4 *a*, 2/*m*..) and six O sites (O2–O5: 8 *f*; O1, O6: 16 *g*, 1) in the asymmetric unit. Compared with $Co_8TeAs_2O_{16}$, sites Co3 and Co4 of $Co_5In_3SbSi_2O_{16}$ are co-occupied by In, the Te site is replaced by Sb, and the As site by Si. Co-occupation of sites by Co and In was also observed for different modifications of Co_2InSbO_6 (Ji *et al.*, 2022) or Co_2InBO_5 and $Co_{3-x}In_xBO_5$ solid solutions (Cai *et al.*, 2014).

The principal building units in the crystal structure of (**I**) are [Co1O_4] and [Si1O_4] tetrahedra and [Co2O_6], [(In1,Co3)O_6],



OPEN ACCESS
Published under a CC BY 4.0 licence

Table 1
Details of the coordination by O atoms around the metal cations and results of BVS calculations.

Site	Coordination number	Range of bond lengths (Å)	Mean bond length (Å)	Mean bond length (literature value) (Å)	BVS (valence units)
Co1	4	1.977 (2)–1.997 (3)	1.984	1.967 (22)[c]	1.86
Co2	6	2.128 (2)–2.1913 (19)	2.147	2.108 (62)[c]	1.82
(In1,Co3)[a]	6	2.078 (3)–2.2745 (19)	2.156	Co 2.108 (62)[c], In 2.142 (42)[d]	2.73
(In2,Co4)[b]	6	2.084 (2)–2.219 (2)	2.137	Co 2.108 (62)[c], In 2.142 (42)[d]	2.53
Sb1	6	1.9818 (19)–1.989 (3)	1.984	1.977 (34)[d]	4.94
Si1	4	1.622 (3)–1.648 (3)	1.630	1.625 (24)[d]	3.94
O1	4 [2Co+Sb+(In,Co)]				1.93
O2	3 [Si+Co+(In,Co)]				1.96
O3	3 [Si+2(In,Co)]				1.97
O4	5 [2Co+3(In,Co)]				1.80
O5	4 (Sb+3Co)				1.90
O6	3 [Si+2(In,Co)]				1.93

Notes: (*a*) In:Co ratio 0.9:0.1; (*b*) In:Co ratio 0.6:0.4; (*c*) Gagné & Hawthorne (2020); (*d*) Gagné & Hawthorne (2018).

[(In2,Co4)O_6] and [Sb1O_6] octahedra. Ranges and averages of bond lengths in these polyhedra comply with literature values and are summarized in Table 1.

The rather complex crystal structure of (**I**) is made up from vertex- and edge-sharing of the building units and is displayed in Fig. 1. As the structural details have already been discussed at length in connection with isotypic $Co_8TeAs_2O_{16}$ (Staack & Müller-Buschbaum, 1997), we will limit ourselves to the most notable features: The [Sb1O_6] octahedra are isolated from others, and a {Co1Si1O_7} double tetrahedron is formed *via* a bridging O atom (O2) and is also isolated from other double tetrahedra. These entities are linked by [100] chains of edge-sharing [CoO_6] and [(In,Co)O_6] octahedra into a framework structure; a fragment of this is shown in Fig. 2.

Bond-valence-sum (BVS) calculations (Brown, 2002) were carried out with the *ECoN21* program (Ilinca, 2022) to validate the structure model. The calculated bond-valence sums (Table 2) of Co1, Co2, Sb1, Si1 and the six O atoms are close to the expected values (in parentheses) for Co (2), Sb (5), Si (4) and O (2) atoms. The mixed-occupied (In1,Co3) and (In2,Co4) sites exhibit BVS values between 2 and 3, which is consistent with the formal charges of +2 for Co and +3 for In, as well as the different In:Co ratio. The strongest deviation from expectation pertains to O4, which is bonded to five metal cations [2Co, 3(In,Co)] and not to the higher-charged Si or Sb atoms. The global instability index (GII) of 0.11 valence units indicates a stable and not particularly strained crystal structure (Salinas-Sanchez *et al.*, 1992; Brown, 2009).

Table 2
Absolute distances |u| (Å) of matching atom pairs, arithmetic mean (d_{av}) of distances (Å), degree of lattice distortion (S) and measure of similarity (δ) in the isotypic crystal structures of $Co_5In_3SbSi_2O_{16}$ and $Co_8TeAs_2O_{16}$.

Co1	0.0523	O1	0.0526
Co2	0.0817	O2	0.1220
(In1,Co3)[a]/Co3	0.0943	O3	0.1195
(In2,Co4)[b]/Co4	0.1057	O4	0.0413
Sb1/Te1	0	O5	0.0243
Si1/As1	0.0489	O6	0.0709
S	0.0050		
d_{av}	0.0694		
δ	0.027		

Notes: (*a*) In:Co ratio 0.9:0.1; (*b*) In:Co ratio 0.6:0.4.

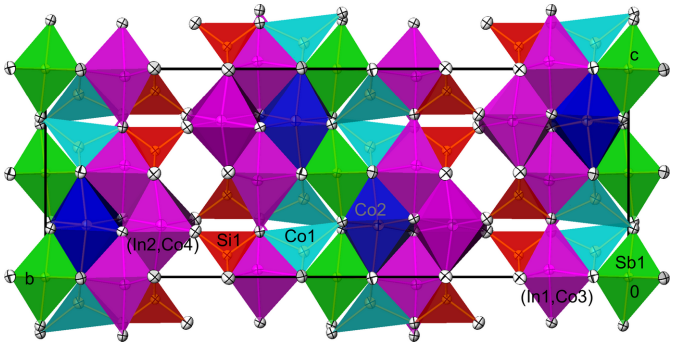


Figure 1
Polyhedral representation of the crystal structure of (**I**) in a view along [$\bar{1}$00]. Displacement ellipsoids are represented at the 90% probability level. Colour codes for polyhedra: Co in tetrahedral coordination is turquoise, Co2 in octahedral coordination is blue, mixed (In,Co) sites in octahedral coordination are pink, antimonate octahedra are green and silicate tetrahedra are red.

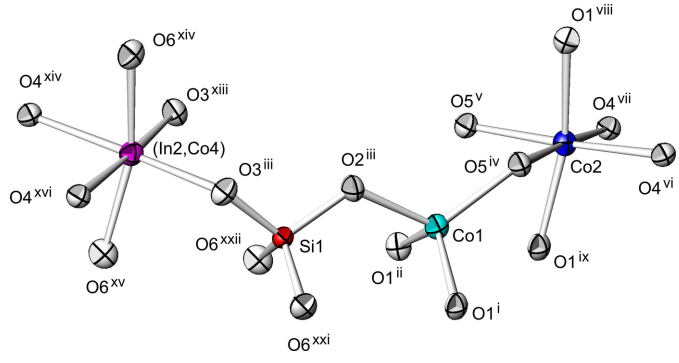


Figure 2
Fragment of the crystal structure showing the {Co1Si1O_7} double tetrahedron linked to [(In2,Co4)O_6] and [Co2O_6] octahedra. Displacement ellipsoids are as in Fig. 1. [Symmetry codes: (i) $x-\frac{1}{2}, y+\frac{1}{2}, z$; (ii) $-x+\frac{1}{2}, y+\frac{1}{2}, z$; (iii) $x, y+\frac{1}{2}, -z+\frac{1}{2}$; (iv) $x, y-\frac{1}{2}, -z+\frac{1}{2}$; (v) $x+\frac{1}{2}, y-\frac{1}{2}, z$; (vi) $-x, -y+\frac{1}{2}, z-\frac{1}{2}$; (vii) $-x+\frac{1}{2}, -y+\frac{1}{2}, -z+1$; (viii) $x, -y+\frac{1}{2}, z+\frac{1}{2}$; (ix) $-x+\frac{1}{2}, -y+\frac{1}{2}, -z$; (xiii) $x+\frac{1}{2}, y+\frac{1}{2}, z$; (xiv) $-x+\frac{1}{2}, -y+1, z-\frac{1}{2}$; (xv) $x, -y+1, -z+1$; (xvi) $-x, -y+1, -z+1$; (xxi) $x-\frac{1}{2}, y+\frac{1}{2}, z-1$; (xxii) $-x+\frac{1}{2}, y+\frac{1}{2}, z-1$.]

Numerical data from a quantitative comparison of the isotypic structures of (**I**) and $Co_8TeAs_2O_{16}$, carried out using the *compstru* program (de la Flor *et al.*, 2016), which is available on the Bilbao Crystallographic Server (Aroyo *et al.*, 2006), are summarized in Table 2. The low values for the degree of lattice distortion (0.0050) and the measure of similarity (0.027) indicate a high degree of similarity between the two crystal structures. The highest differences in atomic positions pertain to atoms O2 and O3, both of which are part of the silicate tetrahedron and two [CoO_6] (for the arsenate) or one [CoO_6] and one [(In,Co)O_6] octahedron (for the silicate). Interestingly, the differences for O4, which is bound to five octahedrally coordinated metal atoms [Co or (In,Co)] but not to the double tetrahedron or the Sb (Te) atom (Table 2), are small.

3. Synthesis and crystallization

$Co_5In_3SbSi_2O_{16}$ formed serendipitously during phase-formation studies in the system Co/In/Sb/O aimed at a phase with composition Co_2InSbO_6 (Ji *et al.*, 2022) by using chemical vapour transport reactions (CVTR; Binnewies *et al.*, 2012). Stoichiometric amounts of Co_3O_4 (Alfa-Aesar, >99%), In_2O_3 (Merck KGaA, >99.5%) and Sb_2O_5 [Thermo Fisher Scientific, 99.998% (metals basis)] were weighted in an 1.333:1:1 ratio (altogether *ca.* 300 mg), intimidately ground in an agate mortar and combined with $HgCl_2$ (60 mg) as the transport agent. The mixture was loaded in a silica ampoule (volume ca. 20 cm^3) that was evacuated, sealed and placed in a two-zone furnace using a gradient 1223 → 1123 K for 4 days. $Co_5In_3SbSi_2O_{16}$ crystallized in the cooler sink side by reacting with the glass ampoule in form of sub-mm blue plates; brown crystals of preliminary composition $Co_8In_{11}Sb_7O_{42}$ were also present at the sink side. Powder X-ray diffraction of the bulk revealed an approximate phase ratio $Co_5In_3SbSi_2O_{16}$:$Co_8In_{11}Sb_7O_{42}$ of 1:9. At the source side, $CoSb_2O_6$ (Reimers *et al.*, 1989) and monoclinic $InSbO_4$ (Wolflehner, 2026) were identified.

An attempt to synthesize $Co_5In_3SbSi_2O_{16}$ specifically under the same conditions as described above, using Co_3O_4, Sb_2O_5, In_2O_3 and SiO_2 (Merck, purum) in the stoichiometric ratio 1.67:0.5:1.5:2, resulted in the formation of $Co_5In_3SbSi_2O_{16}$ crystals as the only product present in the sink region. In the source region, $Co_5In_3SbSi_2O_{16}$, $CoSb_2O_6$ and spinel-type $Co_{2.33}Sb_{0.67}O_4$ (Dulac & Durif, 1960) were identified in an approximate ratio of 5:1:1 according to powder X-ray diffraction of the bulk.

4. Refinement

Crystal data, data collection and structure refinement details are summarized in Table 3. Starting atomic coordinates and the labelling scheme were taken from isotypic $Co_8As_2TeO_{16}$ (Staack & Müller-Buschbaum, 1997). Initial refinement considering two Co, two In, one Sb, one Si and six O sites resulted in the composition $Co_4In_4SbSi_2O_{16}$, i.e. a charged compound under consideration of oxidation states of +II for Co, +III for In, +V for Sb and +IV for Si. Successive free refinement of the site occupation factors of the metal sites revealed full occupation for Co1, Co2, Sb1, Si1, but a minor under-occupation for In1 and a pronounced under-occupation for In2. To achieve charge neutrality, both sites were co-occupied with Co atoms in a fixed In1:Co3 ratio of 0.9:0.1 and In2:Co4 ratio of 0.6:0.4. The remaining maximum and minimum electron densities in the final model are located 0.96 and 0.76 Å, respectively, from Sb1.

Table 3
Experimental details.

Crystal data	
Chemical formula	$Co_5In_3SbSi_2O_{16}$
M_r	1073.04
Crystal system, space group	Orthorhombic, *Cmce*
Temperature (K)	293
a, *b*, *c* (Å)	6.1012 (4), 23.8586 (6), 8.5282 (18)
V (Å^3)	1241.4 (3)
Z	4
Radiation type	Mo *Kα*
μ (mm^{-1})	14.40
Crystal size (mm)	0.10 × 0.08 × 0.05
Data collection	
Diffractometer	Stoe STADIVARI
Absorption correction	Multi-scan (*LANA*; Koziskova *et al.*, 2016)
T_{min}, T_{max}	0.474, 0.874
No. of measured, independent and observed [$I > 2\sigma(I)$] reflections	6885, 1580, 1320
R_{int}	0.032
$(\sin\theta/\lambda)_{max}$ (Å^{-1})	0.834
Refinement	
$R[F^2 > 2\sigma(F^2)]$, $wR(F^2)$, *S*	0.024, 0.056, 1.01
No. of reflections	1580
No. of parameters	75
$\Delta\rho_{max}$, $\Delta\rho_{min}$ (e Å^{-3})	1.54, −2.23

Computer programs: *X-AREA* (Folkers-Karlsson *et al.*, 2026), *SHELXT* (Sheldrick, 2015*a*), *SHELXL* (Sheldrick, 2015*b*), *ATOMS* (Dowty, 2006) and *publCIF* (Westrip, 2010).

Acknowledgements

The authors acknowledge the X-ray Centre of TU Wien for providing access to instrumentation and analysis software and TU Wien Bibliothek for financial support through its Open Access Funding Program.

References

Aroyo, M. I., Perez-Mato, J. M., Capillas, C., Kroumova, E., Ivantchev, S., Madariaga, G., Kirov, A. & Wondratschek, H. (2006). *Z. Kristallogr.* **221**, 15–27.
Binnewies, M., Glaum, R., Schmidt, M. & Schmidt, P. (2012). *Chemical Vapor Transport Reactions* Berlin, Boston: De Gruyter.
Brown, I. D. (2002). *The Chemical Bond in Inorganic Chemistry: The Bond Valence Model.* Oxford University Press.
Brown, I. D. (2009). *Chem. Rev.* **109**, 6858–6919.
Cai, G. M., Wang, L., Su, L. M., Liu, H. S. & Jin, Z. P. (2014). *J. Alloys Compd.* **615**, 809–816.
Dowty, E. (2006). *ATOMS*. Shape Software, Kingsport, Tennessee, USA.
Dulac, J. F. & Durif, A. (1960). *C. R. Hebd. Seances Acad. Sci.* **251**, 747–749.

Flor, G. de la, Orobengoa, D., Tasci, E., Perez-Mato, J. M. & Aroyo, M. I. (2016). *J. Appl. Cryst.* **49**, 653–664.
Folkers-Karlsson, L. C., Celani, P., Hahn, F. & Richter, J. (2026). *Z. Kristallogr.* **241**, 41–51.
Gagné, O. C. & Hawthorne, F. C. (2018). *Acta Cryst.* B**74**, 79–96.
Gagné, O. C. & Hawthorne, F. C. (2020). *IUCrJ* **7**, 581–629.
Ilinca, G. (2022). *Minerals* **12**, 924.
Ivanov, S. A., Mathieu, R., Nordblad, P., Tellgren, R., Ritter, C., Politova, E., Kaleva, G., Mosunov, A., Stefanovich, S. & Weil, M. (2013). *Chem. Mater.* **25**, 935–945.
Ivanov, S., Nordblad, P., Mathieu, R., Tellgren, R., Politova, E. & André, G. (2011). *Eur. J. Inorg. Chem.* pp. 4691–4699.
Ji, K., Solana–Madruga, E., Patino, M. A., Shimakawa, Y. & Attfield, J. P. (2022). *Angew. Chem. Int. Ed.* **61**, e202203062.
Koziskova, J., Hahn, F., Richter, J. & Kožíšek, J. (2016). *Acta Chim. Slovaca* **9**, 136–140.
Reimers, J. N., Greedan, J. E., Stager, C. V. & Kremer, R. (1989). *J. Solid State Chem.* **83**, 20–30.
Salinas-Sanchez, A., Garcia-Muñoz, J. L., Rodriguez-Carvajal, J., Saez-Puche, R. & Martinez, J. L. (1992). *J. Solid State Chem.* **100**, 201–211.
Sheldrick, G. M. (2015*a*). *Acta Cryst.* A**71**, 3–8.
Sheldrick, G. M. (2015*b*). *Acta Cryst.* C**71**, 3–8.
Staack, M. & Müller-Buschbaum, Hk. (1997). *Z. Naturforsch. Teil B* **52**, 643–646.
Weil, M., Mathieu, R., Nordblad, P. & Ivanov, S. A. (2014). *Cryst. Res. Technol.* **49**, 142–151.
Westrip, S. P. (2010). *J. Appl. Cryst.* **43**, 920–925.
Wolflehner, T. (2026). Part of PhD Thesis (unpublished). TU Wien, Austria.

supporting information

Acta Cryst. (2026). E**82**, 1338-1341 [https://doi.org/10.1107/S2056989026010960]

Occupational disorder of cobalt and indium in the crystal structure of $Co_5In_3SbSi_2O_{16}$

Tobias Wolflehner and Matthias Weil

Computing details

Pentacobalt(II) triindium(III) antimony(V) disilicon(VI) hexadecaoxide

Crystal data

$Co_5In_3SbSi_2O_{16}$
M_r = 1073.04
Orthorhombic, *Cmce*
a = 6.1012 (4) Å
b = 23.8586 (6) Å
c = 8.5282 (18) Å
V = 1241.4 (3) Å^3
Z = 4
$F(000)$ = 1956
D_x = 5.741 Mg m^{-3}
Mo $K\alpha$ radiation, λ = 0.71073 Å
Cell parameters from 14765 reflections
θ = 3.4–36.5°
μ = 14.40 mm^{-1}
T = 293 K
Plate, red
0.10 × 0.08 × 0.05 mm

Data collection

Stoe STADIVARI diffractometer
Detector resolution: 13.33 pixels mm^{-1}
rotation method, ω scans
Absorption correction: multi-scan (*LANA*; Koziskova *et al.*, 2016)
T_{min} = 0.474, T_{max} = 0.874
6885 measured reflections
1580 independent reflections
1320 reflections with $I > 2\sigma(I)$
R_{int} = 0.032
θ_{max} = 36.4°, θ_{min} = 3.4°
h = −3→10
k = −39→35
l = −6→14

Refinement

Refinement on F^2
Least-squares matrix: full
$R[F^2 > 2\sigma(F^2)]$ = 0.024
$wR(F^2)$ = 0.056
S = 1.01
1580 reflections
75 parameters
0 restraints
$w = 1/[\sigma^2(F_o^2) + (0.033P)^2]$ where $P = (F_o^2 + 2F_c^2)/3$
$(\Delta/\sigma)_{max}$ = 0.001
$\Delta\rho_{max}$ = 1.54 e Å^{-3}
$\Delta\rho_{min}$ = −2.23 e Å^{-3}

Special details

Geometry. All esds (except the esd in the dihedral angle between two l.s. planes) are estimated using the full covariance matrix. The cell esds are taken into account individually in the estimation of esds in distances, angles and torsion angles; correlations between esds in cell parameters are only used when they are defined by crystal symmetry. An approximate (isotropic) treatment of cell esds is used for estimating esds involving l.s. planes.

Fractional atomic coordinates and isotropic or equivalent isotropic displacement parameters (Å²)

	x	*y*	*z*	U_{iso}*/U_{eq}	Occ. (<1)
Co1	0.000000	0.55684 (2)	0.12353 (6)	0.00899 (10)	
Co2	0.250000	0.42916 (2)	0.250000	0.00861 (10)	
Co3	0.000000	0.13625 (2)	0.03647 (3)	0.00856 (6)	0.1
In1	0.000000	0.13625 (2)	0.03647 (3)	0.00856 (6)	0.9
Co4	0.250000	0.80155 (2)	0.250000	0.00934 (7)	0.4
In2	0.250000	0.80155 (2)	0.250000	0.00934 (7)	0.6
Si1	0.000000	0.68839 (4)	0.10629 (12)	0.00706 (17)	
Sb1	0.000000	0.000000	0.000000	0.00677 (7)	
O1	0.2222 (3)	0.06057 (8)	0.0046 (2)	0.0096 (3)	
O2	0.000000	0.13256 (11)	0.2799 (3)	0.0108 (5)	
O3	0.000000	0.24301 (12)	0.2804 (3)	0.0106 (5)	
O4	0.000000	0.13194 (11)	0.7828 (3)	0.0089 (5)	
O5	0.000000	0.99103 (12)	0.2319 (3)	0.0098 (5)	
O6	0.2821 (3)	0.18631 (8)	0.9968 (2)	0.0107 (4)	

Atomic displacement parameters (Å²)

	U^{11}	U^{22}	U^{33}	U^{12}	U^{13}	U^{23}
Co1	0.00738 (19)	0.0093 (2)	0.0103 (2)	0.000	0.000	0.00064 (18)
Co2	0.00728 (19)	0.0091 (2)	0.0095 (2)	0.000	0.00118 (16)	0.000
Co3	0.00825 (10)	0.00913 (12)	0.00829 (12)	0.000	0.000	−0.00009 (9)
In1	0.00825 (10)	0.00913 (12)	0.00829 (12)	0.000	0.000	−0.00009 (9)
Co4	0.00864 (13)	0.00895 (15)	0.01044 (15)	0.000	−0.00114 (10)	0.000
In2	0.00864 (13)	0.00895 (15)	0.01044 (15)	0.000	−0.00114 (10)	0.000
Si1	0.0067 (4)	0.0072 (4)	0.0073 (4)	0.000	0.000	−0.0004 (4)
Sb1	0.00580 (12)	0.00698 (14)	0.00754 (15)	0.000	0.000	0.00012 (11)
O1	0.0072 (7)	0.0092 (9)	0.0123 (9)	−0.0016 (6)	−0.0006 (6)	0.0005 (8)
O2	0.0142 (12)	0.0076 (12)	0.0106 (13)	0.000	0.000	−0.0005 (10)
O3	0.0086 (10)	0.0106 (12)	0.0124 (13)	0.000	0.000	0.0023 (10)
O4	0.0085 (10)	0.0094 (12)	0.0089 (12)	0.000	0.000	0.0004 (10)
O5	0.0113 (11)	0.0083 (12)	0.0098 (12)	0.000	0.000	−0.0007 (10)
O6	0.0064 (7)	0.0130 (10)	0.0128 (9)	−0.0016 (6)	−0.0016 (6)	0.0010 (8)

Geometric parameters (Å, º)

Co1—O1^{i}	1.977 (2)	In2—O3^{iii}	2.084 (2)
Co1—O1^{ii}	1.977 (2)	In2—O3^{xiii}	2.084 (2)
Co1—O2^{iii}	1.986 (3)	In2—O6^{xiv}	2.1340 (19)
Co1—O5^{iv}	1.997 (3)	In2—O6^{xv}	2.1340 (19)
Co2—O5^{v}	2.128 (2)	In2—O4^{xiv}	2.219 (2)
Co2—O5^{iv}	2.128 (2)	In2—O4^{xvi}	2.219 (2)
Co2—O4^{vi}	2.128 (2)	Sb1—O1^{xvii}	1.9818 (19)
Co2—O4^{vii}	2.128 (2)	Sb1—O1^{xii}	1.9818 (19)
Co2—O1^{viii}	2.1913 (19)	Sb1—O1^{xviii}	1.9818 (19)
Co2—O1^{ix}	2.1913 (19)	Sb1—O1	1.9818 (19)

In1—O2	2.078 (3)	Sb1—O5^{xix}	1.989 (3)
In1—O6^{x}	2.1220 (18)	Sb1—O5^{xx}	1.989 (3)
In1—O6^{xi}	2.1220 (18)	Si1—O3^{iii}	1.622 (3)
In1—O4^{x}	2.165 (3)	Si1—O6^{xxi}	1.6252 (19)
In1—O1	2.2744 (19)	Si1—O6^{xxii}	1.6252 (19)
In1—O1^{xii}	2.2745 (19)	Si1—O2^{iii}	1.648 (3)

O1^{i}—Co1—O1^{ii}	118.00 (11)	O3^{iii}—Si1—O6^{xxii}	111.51 (10)
O1^{i}—Co1—O2^{iii}	99.91 (8)	O6^{xxi}—Si1—O6^{xxii}	109.78 (14)
O1^{ii}—Co1—O2^{iii}	99.91 (8)	O3^{iii}—Si1—O2^{iii}	107.36 (15)
O1^{i}—Co1—O5^{iv}	110.62 (7)	O6^{xxi}—Si1—O2^{iii}	108.28 (10)
O1^{ii}—Co1—O5^{iv}	110.62 (7)	O6^{xxii}—Si1—O2^{iii}	108.28 (10)
O2^{iii}—Co1—O5^{iv}	117.34 (12)	O1^{xvii}—Sb1—O1^{xii}	93.67 (11)
O5^{v}—Co2—O5^{iv}	92.17 (11)	O1^{xvii}—Sb1—O1^{xviii}	86.33 (11)
O5^{v}—Co2—O4^{vi}	176.59 (10)	O1^{xii}—Sb1—O1^{xviii}	180.00 (11)
O5^{iv}—Co2—O4^{vi}	87.25 (7)	O1^{xvii}—Sb1—O1	180.0
O5^{v}—Co2—O4^{vii}	87.25 (7)	O1^{xii}—Sb1—O1	86.33 (11)
O5^{iv}—Co2—O4^{vii}	176.59 (10)	O1^{xviii}—Sb1—O1	93.67 (11)
O4^{vi}—Co2—O4^{vii}	93.54 (11)	O1^{xvii}—Sb1—O5^{xix}	93.38 (8)
O5^{v}—Co2—O1^{viii}	92.86 (9)	O1^{xii}—Sb1—O5^{xix}	86.62 (8)
O5^{iv}—Co2—O1^{viii}	78.17 (9)	O1^{xviii}—Sb1—O5^{xix}	93.38 (8)
O4^{vi}—Co2—O1^{viii}	83.73 (9)	O1—Sb1—O5^{xix}	86.62 (8)
O4^{vii}—Co2—O1^{viii}	105.22 (10)	O1^{xvii}—Sb1—O5^{xx}	86.62 (8)
O5^{v}—Co2—O1^{ix}	78.17 (9)	O1^{xii}—Sb1—O5^{xx}	93.38 (8)
O5^{iv}—Co2—O1^{ix}	92.86 (9)	O1^{xviii}—Sb1—O5^{xx}	86.62 (8)
O4^{vi}—Co2—O1^{ix}	105.22 (10)	O1—Sb1—O5^{xx}	93.38 (8)
O4^{vii}—Co2—O1^{ix}	83.73 (9)	O5^{xix}—Sb1—O5^{xx}	180.00 (17)
O1^{viii}—Co2—O1^{ix}	167.15 (10)	Co1^{v}—O1—Sb1	124.31 (10)
O2—In1—O6^{x}	100.54 (7)	Co1^{v}—O1—Co2^{ix}	116.55 (9)
O2—In1—O6^{xi}	100.54 (7)	Sb1—O1—Co2^{ix}	96.61 (8)
O6^{x}—In1—O6^{xi}	108.41 (10)	Co1^{v}—O1—In1	119.02 (9)
O2—In1—O4^{x}	174.85 (10)	Sb1—O1—In1	99.99 (8)
O6^{x}—In1—O4^{x}	82.40 (7)	Co2^{ix}—O1—In1	94.35 (7)
O6^{xi}—In1—O4^{x}	82.40 (7)	Si1^{iv}—O2—Co1^{iv}	119.41 (17)
O2—In1—O1	94.93 (8)	Si1^{iv}—O2—In1	123.65 (16)
O6^{x}—In1—O1	86.81 (7)	Co1^{iv}—O2—In1	116.94 (14)
O6^{xi}—In1—O1	155.68 (8)	Si1^{iv}—O3—Co4^{iv}	127.76 (8)
O4^{x}—In1—O1	80.96 (7)	Si1^{iv}—O3—Co4^{xxiii}	127.76 (8)
O2—In1—O1^{xii}	94.93 (8)	Co4^{iv}—O3—Co4^{xxiii}	94.07 (12)
O6^{x}—In1—O1^{xii}	155.68 (8)	Co2^{xxiv}—O4—Co2^{vii}	91.56 (11)
O6^{xi}—In1—O1^{xii}	86.81 (7)	Co2^{xxiv}—O4—Co3^{xxv}	99.44 (9)
O4^{x}—In1—O1^{xii}	80.96 (7)	Co2^{vii}—O4—Co3^{xxv}	99.44 (9)
O1—In1—O1^{xii}	73.18 (10)	Co2^{xxiv}—O4—Co4^{xxvi}	164.99 (15)
O3^{iii}—In2—O3^{xiii}	95.85 (12)	Co2^{vii}—O4—Co4^{xxvi}	88.89 (2)
O3^{iii}—In2—O6^{xiv}	98.43 (9)	Co3^{xxv}—O4—Co4^{xxvi}	95.28 (10)
O3^{xiii}—In2—O6^{xiv}	92.02 (9)	Co2^{xxiv}—O4—Co4^{xvi}	88.89 (2)
O3^{iii}—In2—O6^{xv}	92.02 (9)	Co2^{vii}—O4—Co4^{xvi}	164.99 (15)
O3^{xiii}—In2—O6^{xv}	98.43 (9)	Co3^{xxv}—O4—Co4^{xvi}	95.28 (10)

O6^{xiv}—In2—O6^{xv}	164.39 (11)	Co4^{xxvi}—O4—Co4^{xvi}	86.85 (10)
O3^{iii}—In2—O4^{xiv}	176.38 (8)	Sb1^{xxvii}—O5—Co1^{iii}	121.97 (15)
O3^{xiii}—In2—O4^{xiv}	87.73 (7)	Sb1^{xxvii}—O5—Co2^{i}	98.44 (10)
O6^{xiv}—In2—O4^{xiv}	80.88 (9)	Co1^{iii}—O5—Co2^{i}	120.04 (9)
O6^{xv}—In2—O4^{xiv}	87.96 (9)	Sb1^{xxvii}—O5—Co2^{iii}	98.44 (10)
O3^{iii}—In2—O4^{xvi}	87.73 (7)	Co1^{iii}—O5—Co2^{iii}	120.04 (9)
O3^{xiii}—In2—O4^{xvi}	176.38 (8)	Co2^{i}—O5—Co2^{iii}	91.56 (11)
O6^{xiv}—In2—O4^{xvi}	87.96 (9)	Si1^{xxviii}—O6—Co3^{xxv}	126.11 (11)
O6^{xv}—In2—O4^{xvi}	80.88 (9)	Si1^{xxviii}—O6—Co4^{xxvi}	129.60 (11)
O4^{xiv}—In2—O4^{xvi}	88.68 (10)	Co3^{xxv}—O6—Co4^{xxvi}	99.15 (7)
O3^{iii}—Si1—O6^{xxi}	111.51 (10)		

Symmetry codes: (i) $x-1/2, y+1/2, z$; (ii) $-x+1/2, y+1/2, z$; (iii) $x, y+1/2, -z+1/2$; (iv) $x, y-1/2, -z+1/2$; (v) $x+1/2, y-1/2, z$; (vi) $-x, -y+1/2, z-1/2$; (vii) $-x+1/2, -y+1/2, -z+1$; (viii) $x, -y+1/2, z+1/2$; (ix) $-x+1/2, -y+1/2, -z$; (x) $x, y, z-1$; (xi) $-x, y, z-1$; (xii) $-x, y, z$; (xiii) $x+1/2, y+1/2, z$; (xiv) $-x+1/2, -y+1, z-1/2$; (xv) $x, -y+1, -z+1$; (xvi) $-x, -y+1, -z+1$; (xvii) $-x, -y, -z$; (xviii) $x, -y, -z$; (xix) $-x, -y+1, -z$; (xx) $x, y-1, z$; (xxi) $x-1/2, y+1/2, z-1$; (xxii) $-x+1/2, y+1/2, z-1$; (xxiii) $x-1/2, y-1/2, z$; (xxiv) $-x, -y+1/2, z+1/2$; (xxv) $x, y, z+1$; (xxvi) $-x+1/2, -y+1, z+1/2$; (xxvii) $x, y+1, z$; (xxviii) $x+1/2, y-1/2, z+1$.